ChemComm

White-Light Emission from a Structurally Simple Hydrazone

Journal:	*ChemComm*
Manuscript ID	CC-COM-05-2019-003912.R1
Article Type:	Communication

Journal Name

COMMUNICATION

White-Light Emission from a Structurally Simple Hydrazone

Baihao Shao,[a] Nell Stankewitz,[a] Jacob A. Morris,[b] Matthew D. Liptak[b] and Ivan Aprahamian*[a]

Received 00th January 20xx,
Accepted 00th January 20xx

DOI: 10.1039/x0xx00000x

www.rsc.org/

Two hydrazones featuring a unique excitation wavelength-dependent dual fluorescence emission have been developed. The mixing extent of the two emission bands can be modulated by tuning the excitation wavelength resulting in multicolor and even white light emission from structurally simple hydrazones.

Excitation wavelength-dependent fluorescence emission is a sought-after property as it results in fluorophores with tunable optical properties without the need for changes in molecular structure, mixture composition ratio, or molecular interactions.[1] Furthermore excitation-dependent photoluminescence in a single-component system tremendously simplifies device fabrication, thus increasing their practicality and potential use in advanced lighting applications[2] and optical sensing devices. [3] However, and based on Kasha's rule,[4] emission from fluorophores (e.g., organic dyes,[5] inorganic metal complexes[6] and quantum dots[7]) is rarely dependent on excitation wavelength. Nonetheless, effort has been made to discover and elucidate excitation-dependent optical profiles in systems including graphene[8] and its derivatives[9], organic nanoparticles[10] and nanowires[11], carbon nanotubes[12] and nanodots.[13] Quantum confinement effects caused by uneven size distributions[14] lead to the coexistence of discrete electronic transitions of varying energies in such systems, leading to the observed excitation-dependent photoluminescence. Although this phenomenon is relatively common in large scaffolds, it is rarely seen in small molecular architectures (i.e., low molecular weight organic molecules),[15] which are usually easier to access and manipulate synthetically.

Our group is interested in developing functional hydrazone-based materials, ranging from fluorescent dyes[16] to pH and light activated switches.[17] As part of these efforts, we report here on the development of two hydrazones (**1** and **2**; Fig. 1) that exhibit excitation-dependent emission, the linear mixing of which results in the emission of a variety of colors, including white light in the case of **1**. Based on spectral evidence along with fluorescence decay features, we hypothesize that the excitation-dependent emission results from conformational changes that lead to two distinct emissive states in **1** and **2**.[16d,18]

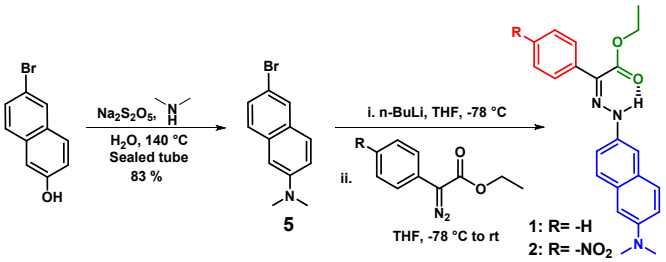

Fig. 1 The synthetic procedure for accessing hydrazones **1** and **2**.

Hydrazones **1** and **2** were synthesized in a straightforward manner, involving in its main step the coupling between 2-diazo-2-phenylacetate or ethyl 2-diazo-2-(4-nitrophenyl) acetate with (6-(dimethylamino) naphthalen-2-yl) lithium under inert conditions (Fig. 1). After column chromatography, **1** and **2** were isolated as orange and red solids in 85 and 25 % yield, respectively, and characterized by NMR spectroscopy (Fig. S4-7, ESI†), mass spectrometry and X-ray crystallography (Fig. S19 and S20, ESI†). Both hydrazones show the characteristic low-field shifted proton signal (δ = 12.4 and 12.7 ppm in CD_3CN, respectively) assignable to the H-bonded (with the carbonyl group) hydrazone N-H proton, implying that they adopt the *Z* configuration in solution. The crystal structures of **1** (N-H···O=C, 2.505(4) Å, 136.22°)[19] and **2** (N-H···O=C, 2.578(2) Å, 135.24°) show that this bond is also persistent in the solid-state.

The photophysical properties of hydrazones **1** and **2** were studied in toluene using UV/Vis and fluorescence spectroscopies. An equilibrated solution of **1** in toluene exhibits a broad absorption band with a maximum (λ_{max}) at 415 nm (ε = 24000 $M^{-1}cm^{-1}$; Fig. 2a).[20] A small shoulder is

[a] *Department of Chemistry, Dartmouth College, Hanover, New Hampshire 03755, USA. E-mail: ivan.aprahamian@dartmouth.edu*
[b] *Department of Chemistry, University of Vermont, Burlington, Vermont 05405, USA.*
Electronic Supplementary Information (ESI) available: [details of any supplementary information available should be included here]. See DOI: 10.1039/x0xx00000x

observed at around λ = 380 nm, indicating the presence of a second electronic transition. Surprisingly, the solution of **1** gives two well-separated emission bands (λ_{em} = 423 and 550 nm) upon excitation (λ_{ex}) at 380 nm (Fig. 2b). This observation led us to explore the emission of **1** under variable excitation wavelengths. When excited at a short wavelength (λ_{ex} = 340 nm) hydrazone **1** exhibits an emission band at 423 nm (Φ_{FL} = 1.09 ± 0.07%), along with a relatively weaker one at 550 nm. Upon switching excitation to a longer wavelength (λ_{ex} = 420 nm) the emission band at 550 nm (Φ_{FL} = 0.10 ± 0.01%) increases in intensity, while the intensity of the band at 423 nm drastically diminishes. Such a variation in emission band as a function of excitation wavelength in small organic compounds is highly unusual. [21]

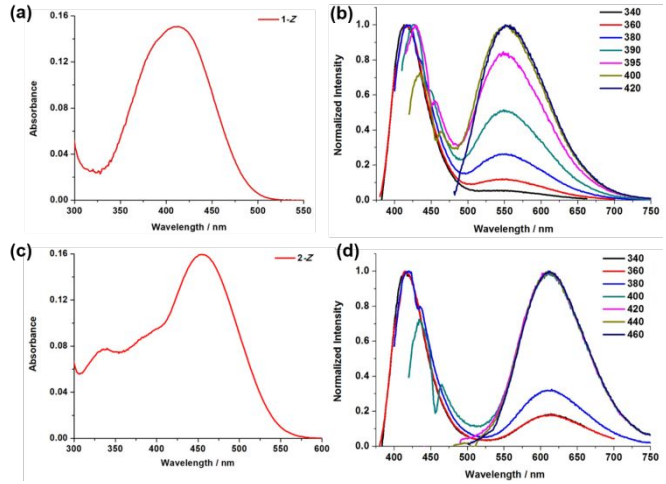

Fig.2 (a) UV/Vis absorption spectrum of **1** (5 × 10^{-6} M) in toluene; (b) Normalized fluorescence emission spectra of **1** (5 × 10^{-6} M) in toluene, under different excitation wavelengths (340 to 420 nm); (c) UV/Vis absorption spectrum of **2** (5 × 10^{-6} M) in toluene; (d) Normalized fluorescence emission spectra of **2** (5 × 10^{-6} M) in toluene, where excitation wavelengths ranging from 340 to 460 nm were applied.

Compared to **1**, compound **2** exhibits a more structured absorption band, which is red-shifted to λ_{max} = 453 nm (ε = 19800 $M^{-1}{\cdot}cm^{-1}$; Fig. 2c) as a result of the push-pull character of the molecule.[22] Moreover, a weaker absorption band at λ_{max} = 340 nm (ε = 8800 $M^{-1}{\cdot}cm^{-1}$) is observed (Fig. 2c) suggesting that there is a second electronic transition in the system. Excitation of **2** with 340 nm light results in an intense emission band at 415 nm (Φ_{FL} = 0.28 ± 0.01%), accompanied with a comparably weak emission at 615 nm (Fig. 2d). When longer wavelengths are used for excitation the intensity of the emission band at 415 nm decreases, whereas the one at 615 nm is enhanced (Φ_{FL} = 0.10 ± 0.01%).

The tunability of the relative intensities of the two emission bands in **1** and **2** allowed us to access multiple color emissions (i.e., other than the blue and red ones mentioned above) from structurally simple molecules.[23] Excitation of **2** at 340 nm leads to a violet color (Fig. 3d) with a CIE coordinate of (0.26, 0.13). Lowering the excitation energy red-shifts the emission band, resulting in a color transition from blue to blue-orange and finally reaching orange red (0.56, 0.42; Fig. 3d). The trend of color changes as a function of excitation energy is summarized in the CIE diagram depicted in Figure 3c, highlighting the accessible range of excitation-dependent multicolor emission.

Unlike compound **2** that features two completely separated fluorescence bands ($\Delta\lambda_{em}$ = 200 nm), compound **1** shows two partially overlapping emission bands (Fig. 2b), which coincidently cover the whole visible range (i.e., 400–700 nm). By tuning the excitation wavelength, the toluene solution of **1** undergoes a color transition from blue (0.19, 0.09) to yellow (0.42, 0.54) (Fig. 3b). As seen in the CIE diagram, **1** exhibits an extensive range of color variation, which covers even the central part of the CIE diagram (i.e., the white light space; Fig. 3a). Excitation of **1** at 395 nm leads to roughly equal intensity emission bands and results in the best coverage of the visible range, leading to white light emission with CIE coordinates of (0.31, 0.35), which is very close to pure white emission (0.33, 0.33).

While we observed fluorescence emission from other hydrazones before,[16f] such an unusual excitation-dependent emission profile is unique to **1** and **2**, which contain a 6-(dimethylamino) naphthalen-2-yl subunit as part of the overall structure. Consequently, we studied (Fig. S13, ESI†) the photophysical properties of the starting naphthyl material (**5**) and realized that it emits blue fluorescence (λ_{em} = 405 nm) upon excitation at 365 nm (λ_{max}). This emission feature corresponds well with the bluish components found in the spectra of **1** and **2** (i.e., 423 nm and 415 nm, respectively). Based on this observation we conclude that the shorter wavelength emission in **1** and **2** mainly emanates from the naphthyl moiety, while the reddish components (i.e., 550 nm and 615 nm) stem from the whole hydrazone, in agreement with previous observations.[16f]

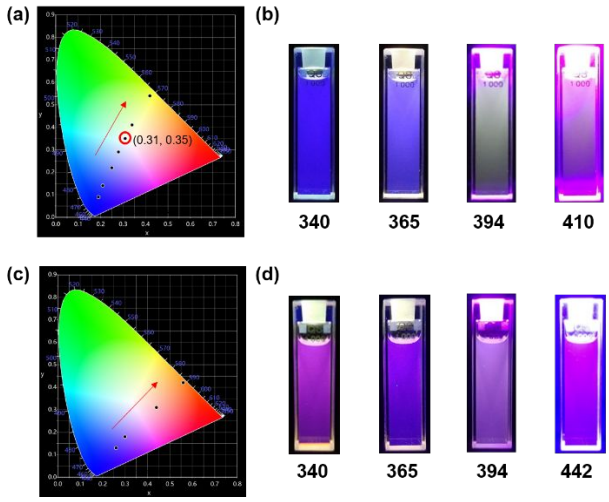

Fig. 3 (a) CIE chromaticity diagram of **1** labelled with CIE coordinates calculated from the spectra in Fig. 2b, where white light (0.31, 0.35) is generated using 395 nm light excitation; (b) Photos of compound **1** in toluene using various excitation wavelengths (i.e., 340, 365, 394 and 410 nm); (c) CIE chromaticity diagram of **2** showing the color changes as a function of excitation wavelength, based on the fluorescence emission spectra shown in Fig. 2d; (d) Selected photos for toluene solutions of **2** under excitation at 340, 365, 394 and 442 nm light. The red arrows in Fig. 3a and 3c represent the changes in CIE coordinates (color variation) as the excitation wavelength shifts bathochromically.

Next, we measured the fluorescence excitation spectra and fluorescence lifetimes of **1** and **2** (using time-correlated single photon counting (TCSPC)) to garner further insights into the nature of the two emissive states. In **1**, the excitation spectrum (λ_{em} = 550 nm; Fig. 4a) corresponds to the absorption band (λ_{max} = 415 nm) confirming the origin of the reddish component in **1**. The excitation spectrum of the bluish component (λ_{em} = 423 nm) of **1** on the other hand has a maximum at 360 nm (Fig. 4a) that does not correspond to bands in the absorption spectrum. Moreover, the two emissions have different fluorescence decay profiles (Fig. S14, S15, and Table S1) illustrating that they originate from different excited states. Similar fluorescence excitation (Fig. 4b) and fluorescence decay profiles (Fig. S16, S17 and Table S1) were measured for the two emissions (λ_{em} = 415 and 615 nm) of compound **2**. The fluorescence excitation spectrum (Fig. 4b) of the 615 nm emission matches the main absorption band (λ_{max} = 453 nm), whereas the other one (λ_{em} = 415 nm) fits the weaker absorption band (λ_{max} = 340 nm) measured in **2**. These results lead us to conclude that there are two distinct emissive states present in hydrazones **1** and **2** giving rise to the excitation wavelength-dependent emission profiles.

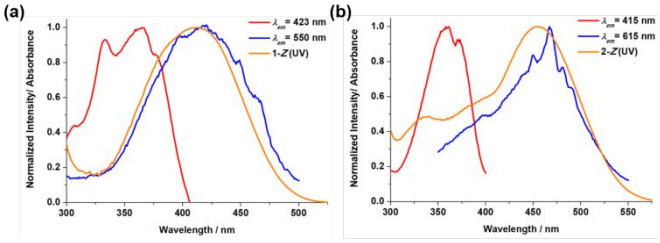

Fig. 4 (a) Normalized UV/Vis spectrum (orange) and fluorescence excitation spectra of **1** in toluene monitored at the emission wavelengths of 423 (red) and 550 nm (blue), respectively; (b) Normalized UV/Vis spectrum (orange) and fluorescence excitation spectra of **2** in toluene monitored at the emission wavelengths of 415 (red) and 615 nm (blue), respectively.

To further elaborate on the nature of the two emissive states we measured the emission spectra of **1** and **2** in toluene at 77K (Figs. S21- S23, ESI†). Neither of the hydrazones exhibits excitation-dependent emission at low temperature, i.e., there is no blue-shifted emission. This result is similar to what happens in the solid-state (Fig. S12, ESI†), i.e., the emission band of **1** in the solid-state (λ_{em} = 570 nm; Φ_{FL} = 3.3 ± 0.1%) does not change upon excitation with different wavelengths of light (340, 394 and 410 nm). We hypothesize that in the rigid environments the hydrazones are locked in a planar conformation (Figs. 19 and 20, ESI†) that prohibits the population of the higher excited state, and hence the blue emission is quenched. This in turn means that in solution, the rotation of the naphthyl fragment, results in a conformation (e.g., perpendicular) that decouples it from the hydrazone core thus populating the higher emissive state and leading to blue emission.

To conclude, we synthesized two structurally simple hydrazone-based fluorophores (**1** and **2**) that exhibit excitation-dependent emission. By fine-tuning the excitation wavelengths, multicolor emissions can be observed in both systems, including white emission in **1**. The different fluorescence decay profiles and excitation spectra of the two emission bands, which are temperature dependent, allow us to conjecture that there are two conformationally accessible emissive states[24] in the hydrazones leading to the excitation-dependent fluorescence property. This unique characteristic of **1** and **2** make them promising candidates for advanced full-color display[25] and ratiometric sensing[26] applications, among others.

Conflicts of interest

There are no conflicts to declare.

Acknowledgements

This work was supported by the generous support of the National Science Foundation (DMR-1506170 for IA, and DMR-1506248 for MDL). N. S. acknowledges the support of the Deutscher Akademischer Austauschdienst (DAAD) RISE program. We are grateful to Prof. Richard Staples (Michigan State University) for the X-ray crystallography data.

Notes and references

1 (a) S. Park, J. E. Kwon, S. H. Kim, J. Seo, K. Chung, S.-Y. Park, D.-J. Jang, B. M. Medina, J. Gierschner, S. Y. Park, *J. Am. Chem. Soc.*, 2009, **131**, 14043−14049; (b) M. Balter, S. Li, M. Morimoto, S. Tang, J. Hernando, G. Guirado, M. Irie, F. M. Raymo, J. Andreasson, *Chem. Sci.*, 2016, **7**, 5867–5871; (c) Q.-W. Zhang, D. Li, X. Li, P. B. White, J. Mecinovic, X. Ma, H. Agren, R. J. M. Notle, H. Tian, *J. Am. Chem. Soc.*, 2016, **138**, 13541−13550; (d) W.-C. Geng, Y.-C. Liu, Y.-Y. Wang, Z. Xu, Z. Zheng, C.-B. Yang, D.-S. Guo, *Chem. Commun.*, 2017, **53**, 392–395; (e) M. Zhang, S. Yin, J. Zhang, Z. Zhou, M. L. Saha, C. Lu, P. J. Stang, *Proc. Natl. Acad. Sci. USA*, 2017, **114**, 3044–3049; (f) L. Mao, Y. Wu, C. C. Stoumpos, M. R. Wasielewski, M. G. Kanatzidis, *J. Am. Chem. Soc.*, 2017, **139**, 5210−5215; (g) Q. Zhao, Y. Chen, S.-H. Li, Y. Liu, *Chem. Commun.*, 2018, **54**, 200–203; (h) W. Zhou, Y. Chen, Q. Yu, P. Li, X. Chen, Y. Liu, *Chem. Sci.*, 2019, **10**, 3346–3352; (i) H. Wu, Y. Chen, X. Dai, P. Li, J. F. Stoddart, Y. Liu, *J. Am. Chem. Soc.*, 2019, **141**, 6583−6591.
2 (a) E. Kim, S. B. Park, *Chem. Asian J.*, 2009, **4**, 1646–1658; (b) S. Mukherjee, P. Thilagar, *Dyes and Pigments*, 2014, **110**, 2–27.
3 (a) L. Basabe-Desmonts, D. N. Reinhoudt, M. Crego-Calama, *Chem. Soc. Rev.*, 2007, **36**, 993−1017; (b) K. P. Carter, A. M. Young, A. E. Palmer, *Chem. Rev.*, 2014, **114**, 4564–4601.
4 M. Kasha, *Discuss. Faraday Soc.*, 1950, **9**, 14−19.
5 (a) A. Loudet, K. Burgess, *Chem. Rev.*, 2007, **11**, 4891–4932; (b) M. Beija, C. A. M. Afonso, J. M. G. Martinho, *Chem. Soc. Rev.*, 2009, **38**, 2410–2433; (c) V. S. Padalkar, S. Seki, *Chem. Soc. Rev.*, 2016, **45**, 169–202.
6 (a) P. Coppo, M. Duati, V. N. Kozhevnikov, J. W. Hofstraat, L. De Cola, *Angew. Chem. Int. Ed.*, 2005, **44**, 1806–1810; (b) M. R. Gill, J. A. Thomas, *Chem. Soc. Rev.*, 2012, **41**, 3179–3192.
7 (a) J. Berezovsky, M. Ouyang, F. Meier, D. D. Awschalom, D.

Battaglia, X. Peng, *Phys. Rev. B*, 2005, **71**, 081309(R); (b) A. P. Beyler, L. F. Marshall, J. Cui, X. Brokmann, M. G. Bawendi, *Phys. Rev. Lett.*, 2013, **111**, 177401.
8 A. Naga, A. Mitra, S. C. Mukhopadhyaya, *Sensors and Actuators, A*, 2018, **270**, 177–194.
9 (a) S. K. Cushing, M. Li, F. Huang, N. Wu, *ACS Nano*, 2014, **8**, 1002–1013; (b) S. K. Cushing, W. Ding, G. Chen, C. Wang, F. Yang, F. Huang, N. Wu, *Nanoscale*, 2017, **9**, 2240–2245.
10 K-M. Lee, W-Y. Cheng, C-Y. Chen, J-J. Shyue, C-C. Nieh, C-F. Chou, J-R. Lee, Y-Y. Lee, C-Y. Cheng, S. Y. Chang, T. C. Yang, M-C. Cheng, B-Y. Lin, *Nat. Commun.*, 2013, **4**, 1544.
11 H. Zhang, X. Xu, H. Ji, *Chem. Commun.*, 2010, **46**, 1917–1919.
12 (a) J. Zhou, C. Booker, R. Li, X. Zhou, T. Sham, X. Sun, Z. Ding, *J. Am. Chem. Soc.*, 2007, **129**, 744–745; (b) I. Khan, S. Huang, C. Wu, *New J. Phys.*, 2017, **19**, 123016.
13 A. Sharma, T. Gadly, A. Gupta, A. Ballal, S. K. Ghosh, M. Kumbhakar, *J. Phys. Chem. Lett.*, 2016, **7**, 3695−3702.
14 S. K. Cushing, W. Ding, G. Chen, C. Wang, F. Yang, F. Huang, N. Wu, *Nanoscale*, 2017, **9**, 2240–2245.
15 (a) G. Eber, F. Grüneis, S. Schneider, F. Dörr, *Chem. Phys. Lett.*, 1974, **29**, 397–404; (b) T. Ito, *Chem. Rev.*, 2012, **112**, 4541−4568.
16 (a) Y. Yang, X. Su, C. Carroll, I. Aprahamian, *Chem. Sci.*, 2012, **3**, 610–613; (b) X. Su, M. D. Liptak, I. Aprahamian, *Chem. Commun.*, 2013, **49**, 4160–4162; (c) H. Qian, I. Aprahamian, *Chem. Commun.*, 2015, **51**, 11158–11161; (d) H. Qian, E. M. Cousins, E. H. Horak, A. Wakefield, M. D. Liptak, I. Aprahamian, *Nat. Chem.*, 2017, **9**, 83–87; (e) H. Qian, B. Shao, I. Aprahamian, *Tetrahedron*, 2017, **73**, 4901–4904; (f) B. Shao, M. Baroncini, H. Qian, L. Bussotti, M. Di Donato, A. Credi, I. Aprahamian, *J. Am. Chem. Soc.*, 2018, **140**, 12323–12327.
17 (a) S. M. Landge, I. Aprahamian, *J. Am. Chem. Soc.,* 2009, **131**, 18269–18271; (b) Y. Yang, R. P. Hughes, I. Aprahamian, *J. Am. Chem. Soc.*, 2012, **134**, 15221–15224; (c) H. Qian, S. Pramanik, I. Aprahamian, *J. Am. Chem. Soc.*, 2017, **139**, 9140–9143; (d) Q. Li, H. Qian, B. Shao, R. P. Huges, I. Aprahamian, *J. Am. Chem. Soc.*, 2018, **140**, 11829−11835; (e) M. J. Moran, M. Magrini, D. M. Walba, I. Aprahamian, *J. Am. Chem. Soc.*, 2018, **140**, 13623−13627; (f) A. Ryabchun, Q. Li, F. Lancia, I. Aprahamian, N. Katsonis, *J. Am. Chem. Soc.*, 2019, 141, 1196−1200; (g) B. Shao, H. Qian, Q. Li, I. Aprahamian, *J. Am. Chem. Soc.* 2019, **141**, 8364−8371.
18 Y. Zhou, G. Baryshnikov, X. Li, M. Zhu, H. Agren, L. Zhu, *Chem. Mater.*, 2018, **30**, 8008–8016;
19 There is disorder at the naphthyl ring in **1** (Fig. S19) resulting in another H-bond with slightly different bonding values (N-H···O=C, 2.82(1) Å, 124.11°).
20 The photochromic behaviour of **1** and **2** was also studied and both molecules exhibited low photoswitching efficiencies (Fig. S8-11, ESI†), and hence, their photoswitching properties were not studied further.
21 (a) Y. Yang, M. Lowry, C. M. Schowalter, S. O. Fakayode, J. O. Escobedo, X. Xu, H. Zhang, T. J. Jensen, F. R. Fronczek, I. M. Warner, R. M. Strongin, *J. Am. Chem. Soc.*, 2006, **43**, 14081–14092; (b) G. He, D. Guo, C. He, X. Zhang, X. Zhao, C. Duan, *Angew. Chem. Int. Ed.*, 2009, **48**, 6132–6135; (c) P. Nandhikonda, M. D. Heagy, *Chem. Commun.*, 2010, **46**, 8002–8004.
22 F. Bureš, *RSC Adv.*, 2014, **4**, 58826–58851.
23 Elemental analysis (see ESI†) verified that the dual-emission profile is not caused by impurities.
24 (a) T. Forster, *Discuss. Faraday Soc.*, 1959, **27**, 7–16; (b) K. E. Sapsford, L. Berti, I. L. Medintz, *Angew. Chem. Int. Ed.*, 2006, **45**, 4562–4588.
25 W. Tian, J. Zhang, J. Yu, J. Wu, J. Zhang, J. He, F. Wang, *Adv. Funct. Mater.*, 2018, **28**, 1703548.
26 M. H. Lee, J. S. Kim, J. L. Sessler, *Chem. Soc. Rev.*, 2015, **44**, 4185–4191.

Journal Name

COMMUNICATION

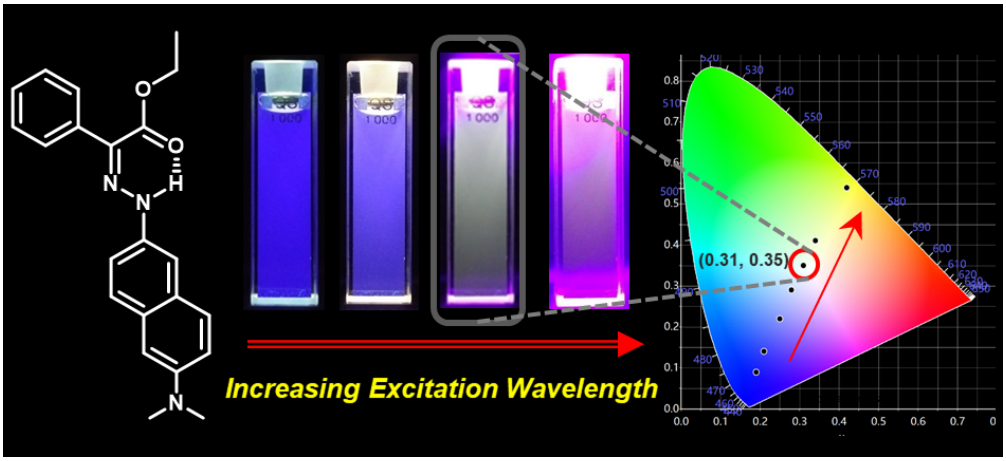

80x36mm (300 x 300 DPI)